Molecular imaging of postprandial metabolism

J Appl Physiol 124: 504–511, 2018.
First published May 11, 2017; doi:10.1152/japplphysiol.00212.2017.

REVIEW | *Imaging in Metabolic Research*

Molecular imaging of postprandial metabolism

Vera B. Schrauwen-Hinderling[1] and André C. Carpentier[2]

[1]*Department of Radiology and Human Biology and Human Movement Sciences, Maastricht University Medical Center, Maastricht, The Netherlands; and* [2]*Department of Medicine, Centre de Recherche du Centre Hospitalier Universitaire de Sherbrooke, Université de Sherbrooke, Sherbrooke, Québec, Canada*

Submitted 8 March 2017; accepted in final form 8 May 2017

Schrauwen-Hinderling VB, Carpentier AC. Molecular imaging of postprandial metabolism. *J Appl Physiol* 124: 504–511, 2018. First published May 11, 2017; doi:10.1152/japplphysiol.00212.2017.—Disordered postprandial metabolism of energy substrates is one of the main defining features of prediabetes and contributes to the development of several chronic diseases associated with obesity, such as type 2 diabetes and cardiovascular diseases. Postprandial energy metabolism has been studied using classical isotopic tracer approaches that are limited by poor access to splanchnic metabolism and highly dynamic and complex exchanges of energy substrates involving multiple organs and systems. Advances in noninvasive molecular imaging modalities, such as PET and MRI/magnetic resonance spectroscopy (MRS), have recently allowed important advances in our understanding of postprandial energy metabolism in humans. The present review describes some of these recent advances, with particular focus on glucose and fatty acid metabolism in the postprandial state, and discusses current gaps in knowledge and new perspectives of application of PET and MRI/MRS for the investigation and treatment of human metabolic diseases.

dietary fat; glucose; energy metabolism; positron emission tomography; magnetic resonance imaging; magnetic resonance spectroscopy

INTRODUCTION

The postprandial state is defined as the period following meal intake. It is characterized by net input of energy substrates and other nutrients from the gastrointestinal track into the splanchnic and systemic circulation. It is thus under normal circumstances, an anabolic state also characterized by complex neurohormonal responses and dynamic changes in blood substrate appearance and disappearance rates. Its duration is variable depending on the digestive rate of the substrate and its downstream metabolism, for example, ranging from 3 to 4 h (10) for glucose, in most instances, to >6 h for dietary fatty acid metabolism (30). Because most individuals eat three or more meals per day, it follows that humans are spending most of the time in the postprandial state, at least with regards to dietary fat metabolism. However, physiological measurements are most often performed in the fasted state to ensure standardization, when metabolic abnormalities are often not apparent. Metabolic disorders often become evident only after a metabolic challenge, for example, after a meal.

By definition, impaired glucose tolerance is an exaggerated postprandial blood glucose excursion. It is a main risk factor for the development of type 2 diabetes and a major defining feature of prediabetes (1). Impaired glucose tolerance and type 2 diabetes are also associated with other disordered postprandial responses of energy substrate metabolism, such as plasma nonesterified fatty acids (NEFAs) and triglycerides (7, 44), amino acids (2), and ketone bodies and lactate (15). As such, the natural history spectrum, from prediabetes to overt type 2 diabetes, displays a varying degree of metabolic inflexibility of different energy substrates from the fasting to the postprandial state, leading to disordered postprandial metabolic responses, including that of fatty acids, amino acids, and glucose itself, demonstrated to play significant roles in the development of type 2 diabetes and many of its end-organ complications, including atherosclerosis, heart failure, and kidney dysfunction (6, 18, 38, 55, 57).

Isotopic tracer studies, using the classical blood or plasma dilution techniques and various modeling methods, have provided important advances in knowledge of postprandial glucose, NEFA, dietary fatty acid, and amino acid metabolism in physiological and pathophysiological conditions. For example, simultaneous intravenous and prandial administration of tracers have quantified the contribution of endogenous vs. exogenous substrate appearance to a postprandial metabolism (37, 43). Breath sampling with determination of isotopic labeling of CO_2 has allowed quantification of dietary and endogenous substrate whole-body oxidation rates (43, 44). Administration of fatty acid tracers with arteriovenous sampling and/or adipose tissue biopsies has also provided in-

Address for reprint requests and other correspondence: A. C. Carpentier, Centre de Recherche du Centre Hospitalier Universitaire de Sherbrooke, Université de Sherbrooke, Sherbrooke, Québec, Canada J1H 5N4 (e-mail: andre.carpentier@usherbrooke.ca).

sight into dietary fatty acid adipose tissue storage (7, 39, 40, 54). However, the study of the postprandial state has been very challenging, even using these state-of-the-art approaches, given their incapacity to monitor directly the digestive and absorptive metabolism of substrate, their limited access to the splanchnic circulation, the incapacity to monitor many organs simultaneously, and severely limited time resolution and repeatability of most of these approaches. Postprandial energy substrate metabolism is dynamic (i.e., highly time dependent), has a variable latent period in usually inaccessible compartments (i.e., gastrointestinal tract and splanchnic circulation), and often involves multiple organs that contribute to the disappearance but also in some instances, to recirculation of these substrates (i.e., liver for glucose and adipose tissues for dietary fatty acids; see below).

Major advances have been made in noninvasive molecular imaging methods over the past decades, allowing for the study of glucose, fatty acid, and amino acid metabolism. With the allowance of noninvasive access to virtually all organ-system metabolisms with higher time resolution and repeatability, these newer tools circumvent many of the limitations of classical tracer methods. Two of these imaging modalities have been particularly useful for the study of energy substrate metabolism in humans: *1*) PET and *2*) MRS/magnetic resonance spectroscopy (MRS; Fig. 1).

PET is based on detection of the two simultaneous gamma photons, emitted almost in the opposite direction, when a positron meets an electron and disintegrates. This unique property of positron-emitting radionuclides (carbon-11 or ^{11}C, nitrogen-13 or ^{13}N, oxygen-15 or ^{15}O, fluorine-18 or ^{18}F, gallium-68 or ^{68}Ga, zirconium-89 or ^{89}Zi, rubidium-82 or ^{82}Ru, and others) potentially allows for accurate localization of the disintegration event along a straight line (or line of response) using two gamma detectors aligned around the subject, provided that the resolving time of the detectors is small enough (typically <500 ps). This allows for more precise three-dimensional reconstruction of coincident gamma photon detection events and the highest sensitivity of PET reaching the picomolar range compared with other radionuclide imaging modalities and MRS (in the millimolar range) (41). This exquisite molecular sensitivity of PET permits the use of very small doses of tracers having very highly specific activity (i.e., radioactivity divided by the mass of tracer). This makes PET an optimal tracer technique in most instances (and certainly in all instances for the study of energetic substrates, such as glucose and fatty acids, found in large concentrations in circulation), as the tracer-to-tracee ratio is minimized (an assumption of the tracer-dilution model). Although PET is an excellent method to track exogenous tracers, the strength of MRS is to detect and quantify endogenous metabolites and monitor the physiological response upon a meal challenge. The high sensitivity of PET makes it possible to use molecules in minute PET-tracer doses [e.g., 18-fluorodeoxyglucose (^{18}FDG) and 18-fluorothiaheptadecanoic acid (^{18}FTHA)], which would perturb the metabolic processes under study and have harmful metabolic effects at large doses (^{18}FDG competitively blocks glycolysis, and ^{18}FTHA competitively blocks fatty acid metabolism). Combined with the relatively large array of positron-emitting radionuclides, this allows for theoretically unlimited versatility of PET tracers with different properties to study any biological process. For example, the glucose metabolism can be studied using ^{11}C-glucose, which is metabolized exactly as endogenous glucose (i.e., tissue uptake and cellular metabolic pathways are all at tracee rates), or using ^{18}FDG, which is taken up by tissues at approximately the same rate as glucose but not metabolized beyond the first phosphorylation step (i.e., mediated by glucokinase or hexokinase) in cells (52, 56). Thus ^{11}C-glucose is ideal to study the glucose oxidative and nonoxidative metabolism, whereas ^{18}FDG is ideal to measure integrated uptake of glucose in tissues over time, improving the detection and imaging of some organs or structures, such as brown adipose tissues (8, 12, 50, 53, 62, 67).

Two acquisition modalities are used for PET metabolic imaging: *1*) whole body ("static scanning") and *2*) dynamic acquisition (Fig. 2). The first is the most commonly used acquisition modality and serves for anatomical detection of structures (i.e., tumors) or the determination of relative uptake (biodistribution or partitioning, usually quantified as "standard uptake value") of the PET tracer. Static scanning is typically used with tracers displaying delayed tissue metabolic clearance, such as ^{18}FDG or ^{18}FTHA, allowing the comparison of the cumulative tracer uptake among different tissues throughout the whole body. It may give precise measurement of relative integrated uptake of the tracee among tissues but cannot precisely determine quantitative fluxes in and out of the tissues. Dynamic scanning, on the other hand, directly measures fluxes in and out of tissues. It is, however, more fastidious to perform, requiring relatively long acquisition scans targeted to a limited anatomic area (i.e., the field of view of the scanner, typically <24 cm along the axis of the body); determination of a blood tracer and metabolite concentrations; and modelization of the data using linearization, compartmental modeling, or spectral analysis (11, 51, 60, 61).

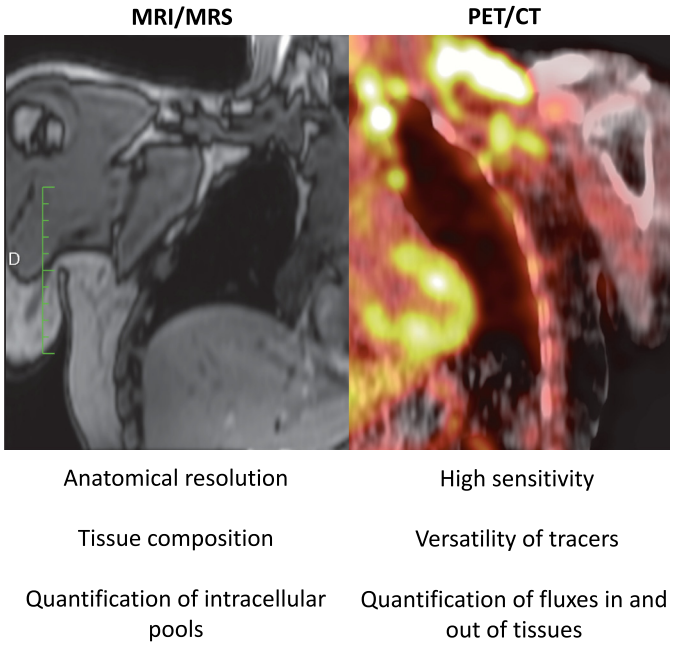

Fig. 1. Complementary strengths of MRI/magnetic resonance spectroscopy (MRS) and PET/computed tomography (CT) for postprandial metabolic imaging.

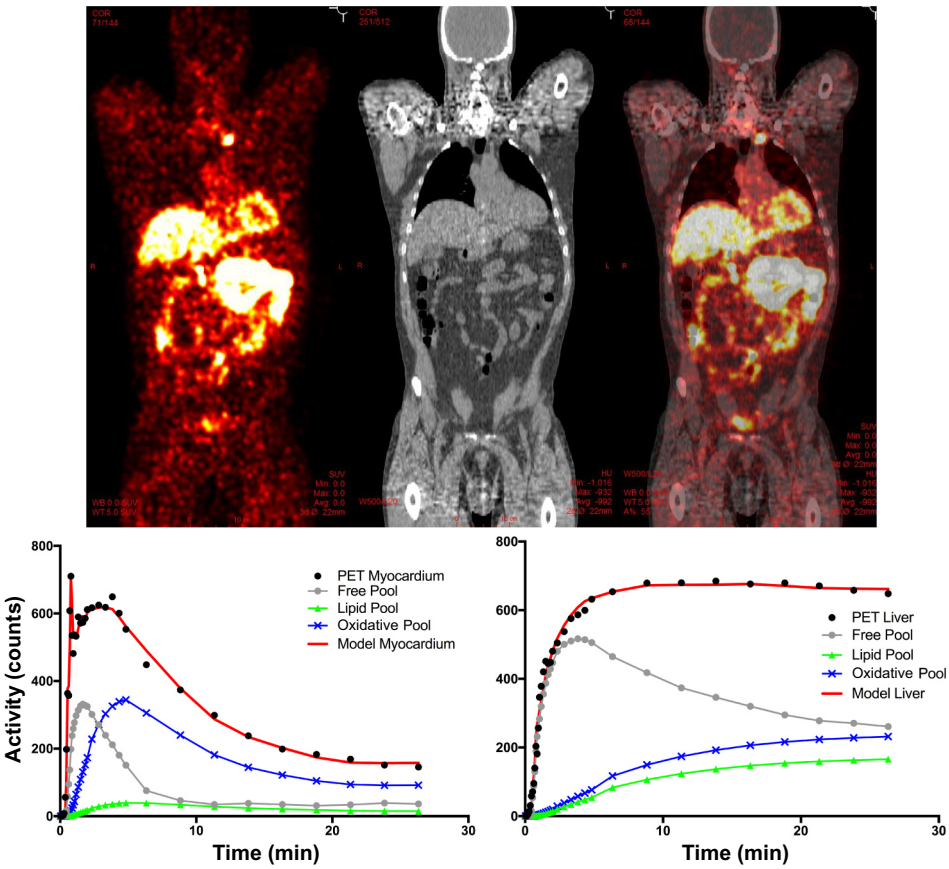

Fig. 2. Whole-body PET (*top left*) coupled to low-dose computed tomography (CT; *top middle*) with merged PET-CT images (*top right*) after oral administration of 18-fluorothiaheptadecanoic acid (^{18}FTHA) in a healthy subject, with examples of multicompartmental modeling of PET dynamic acquisition in list mode after intravenous injection of ^{11}C-palmitate to determine cardiac (*bottom left*) and liver (*bottom right*) oxidative and nonoxidative nonesterified fatty acid metabolism. PET/CT oral ^{18}FTHA data are from a participant of a previously published study (28). ^{11}C-Palmitate dynamic PET data are from an unpublished study, using multicompartmental models from de Jong et al. (13) for the heart and Iozzo et al. (20) for the liver.

The major drawbacks of PET are its high cost; the need for synthesis of the PET tracers on site in most instances, given the very short radioactive half-life of most positron-emitting radionuclides (a few minutes to a few hours); and radioactivity exposure of the participants. The latter severely limits the capacity to repeat measurements over time using this approach. All positron-emitting radionuclides emit the gamma photon of the same energy level, limiting the capacity to perform simultaneous acquisitions using two or more PET tracers. Finally, the relatively low PET spatial resolution results in partial volume effects with signal spillover of surrounding structures, making impossible some measures (e.g., epicardial adipose tissue fatty acid uptake because of very high relative myocardial uptake) and rendering mathematical corrections of the data essential for quantification purposes (11).

The potential of MRS as a complementary method to PET is excellent, as it can accurately determine endogenous concentrations of metabolites and monitor their response upon consumption of a meal. MRS makes use of a property that certain nuclei possess, which is termed "spin" and which results in a measurable net magnetization when exposed to the strong magnetic field in an MRI scanner. Several nuclei have this spin characteristic. The most interesting nuclei for metabolic research are hydrogen (^{1}H), phosphorous (^{31}P), and carbon (^{13}C). Therefore, metabolites that contain hydrogen, phosphorous, or carbon atoms can be detected if they are freely mobile and present in millimolar concentrations. The resonance frequency of nuclei can shift depending on the presence of surrounding chemical liaisons, allowing for the identification and quantification of chemical groups using the area under the peak of the spectrum, which is directly proportional to the concentration. The easiest way for quantification is the use of an internal reference with known concentration (for example, water or creatine). For such relative quantification, the ratio of metabolite/reference suffices to deduce tissue concentrations in millimolars per kilogram. For protons, the most abundant metabolites in human tissue are water and lipids, and an important application of ^{1}H-MRS in metabolic research is the quantification of muscle and liver fat content (intramyocellular lipids and intrahepatic lipids; Fig. 3). In addition, creatine and choline can typically be detected (e.g., in muscle tissue), and when spectral editing is performed, many more metabolites, such as acetylcarnitine or lactate, can be detected. In fact, future development of new MR editing sequences will facilitate the detection and quantification of yet-unobservable metabolites. The field of ^{31}P-MRS mainly focuses on the investigation of energy metabolism, as high-energy metabolites, such as ATP and creatine phosphate, can be quantified. ^{13}C-MRS has been mostly applied to determine glycogen concentrations; however, applications of ^{13}C-MRS can potentially be much broader. Most carbon atoms have a mass number of 12, whereas only carbon nuclei with a mass number of 13 possess spin, and therefore, only these yield an MRS signal. The natural abundance of ^{13}C is only 1.1%, and together with the low sensitivity of ^{13}C-MRS, this is severely limiting signal intensity. However, the low natural abundance of ^{13}C also has advantages, as ^{13}C-labeled substrates can be used as stable (nonradioactive) tracers in

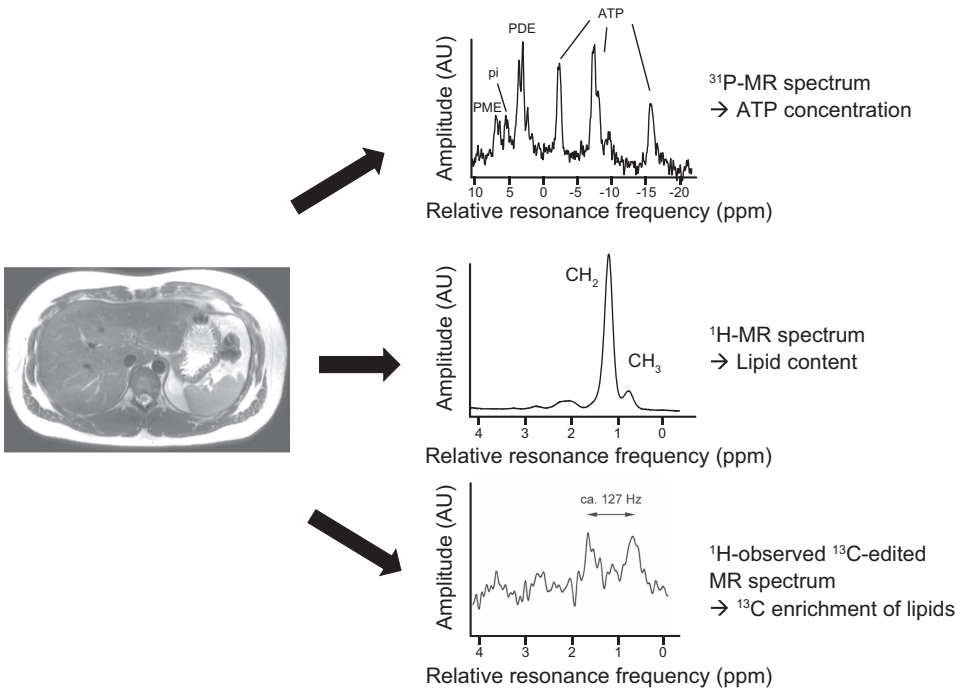

Fig. 3. Axial MRI of the liver (*left*) with a phosphorus-31 (^{31}P) magnetic resonance (MR) spectrum showing high-energy phosphate metabolites (*top right*), a proton (^{1}H) MR spectrum showing liver fat content (*middle right*), and a proton-observed carbon-13 (^{13}C)-edited MR spectrum to determine deposition of ^{13}C-labeled dietary fatty acids in the liver (*lower right*). PDE, phosphodiester; pi, inorganic phosphate; PME, phosphomonoester; ppm, parts per million.

investigating metabolism (see MOLECULAR IMAGING OF POSTPRANDIAL FATTY ACID METABOLISM).

MOLECULAR IMAGING OF POSTPRANDIAL GLUCOSE METABOLISM

Postprandial glucose metabolism, including the contribution of exogenous vs. endogenous glucose appearance to systemic glucose metabolism, has been very well studied using conventional tracers (10, 37). Molecular imaging approaches using PET have been used far less to determine the organ-specific glucose metabolism during the postprandial state. Postprandial metabolic glucose imaging by PET is complicated by at least three important factors: *1*) dynamic changes in insulin and incretin hormones; *2*) changes in circulating fluxes of fatty acids that metabolically compete with glucose uptake and metabolism, at least in some organs; and *3*) postprandial increase in circulating glucose level.

Insulin can increase organ-specific glucose uptake and metabolism directly through stimulation of cell membrane glucose transport and downstream metabolism and indirectly by modification of systemic metabolic rates of other substrates, especially through reduction of circulating NEFA. Insulin is known to increase glucose uptake in the heart (17, 27), skeletal muscles (46), liver (21, 22), brain (19), and adipose tissue depots (23, 63), including brown adipose tissues (47). Organ-specific, insulin-stimulated glucose uptake is, however, strongly determined by insulin-mediated suppression of plasma NEFA (26, 45). Glucagon-like peptide 1 has also been shown to reduce blood-brain glucose transport using ^{18}FDG PET (33).

^{18}FDG PET has been used for cardiac, brain, and brown adipose tissue imaging during the postprandial state. For example, the postprandial biodistribution of circulating glucose between brown and white adipose tissues and lean organs using ^{18}FDG PET has been described and compared with that during acute cold exposure [which activates brown adipose tissue thermogenesis (49)] in healthy men, showing lower brown adipose tissue and higher skeletal muscle glucose uptake in the cold vs. postprandial state (64). However, when compared with the fasting state, brown adipose tissue glucose uptake appears to be lower in the postprandial state (66). This likely results from metabolic competition from dietary fatty acids, as we recently showed that these substrates can be directly used by brown adipose tissues in humans (5). Meals are, on occasion, used to modify organ glucose uptake to the benefit of ^{18}FDG PET clinical investigations. For example, high-fat meals are frequently used to suppress physiological cardiac glucose uptake (through metabolic competition from dietary fatty acids; see MOLECULAR IMAGING OF POSTPRANDIAL FATTY ACID METABOLISM) in preparation for ^{18}FDG PET examination for myocardial inflammation or infection or to detect arterial inflammation (14, 48).

Some aspects of postprandial glucose metabolism can also be investigated with MRS. For example, glycogen concentrations can be determined in the liver and in skeletal muscle before and after meals, and therefore, net glycogen storage after a meal can be determined. With the use of this method, it has been shown that glycogen concentration in muscle is increased by 17% in healthy volunteers after a series of three meals, whereas glycogen concentration in patients with type 2 diabetes mellitus remains unchanged, illustrating a disturbed glycogen storage in muscle in the diabetic state (36). In the liver, glycogen concentrations were also increased after the meals, but here, this postprandial response is not blunted in type 2 diabetes (36). Net glycogen storage can also be determined after a single meal, and peak glycogen concentrations in the liver were found at 3–4 h after a meal (3). Furthermore, it is reported that a meal with a high glycemic index leads to more pronounced postprandial glycogen storage when compared with a meal with a low glycemic index (3).

MOLECULAR IMAGING OF POSTPRANDIAL FATTY ACID METABOLISM

Hepatic fat content can be monitored by ^{1}H-MRS (Fig. 3), and it was shown that 2–3 h after a high-fat, high-energetic meal, hepatic fat content is increased by 13–20% in healthy, lean subjects, indicating net hepatic fat storage after a meal (16, 35). Hepatic fat content was also shown to remain elevated at 5 h after the meal (35). On the other hand, lipid content in skeletal muscle remained unchanged in the postprandial state. Whereas ^{1}H-MRS is broadly applied for monitoring total lipid content in several organs, no information of the source of fat is gained, as endogenous and exogenous fatty acid sources cannot be differentiated. In that respect, ^{13}C-MRS offers unique possibilities, as due to the low background of the ^{13}C signal (natural abundance of ^{13}C is 1.1%), the ^{13}C-labeled substrate can be used as tracers, the signal of which can then be followed in vivo. In that way, the substrate can be tracked, and uptake and turnover can be monitored. For example, ^{13}C-labeled fatty acids were added to a meal, and the ^{13}C lipid signal could be monitored in the liver (34). However, the big challenge in such experiments is the low sensitivity of ^{13}C-MRS and possible contamination of the measured signal from the ^{13}C lipid signal from adipose tissues. Therefore, to realize such experiments, specialized MRS sequence development was necessary to obtain good localization of the ^{13}C signal and a sufficient signal-to-noise ratio to monitor the ^{13}C lipid signal in time. This was possible by implementation of an indirect method to detect ^{13}C-labeled lipids by selectively retaining the ^{1}H signal of ^{13}C-coupled spins (Fig. 3). This strategy makes use of the higher sensitivity of ^{1}H-MRS compared with ^{13}C, to be able to pick up the small differences in the ^{13}C signal. With the use of this method, it was shown that fatty acids, originating from a mixed liquid meal, indeed accumulate in the liver in the first 3–5 h after a meal and that this is the case in lean as well as in overweight to obese subjects (34).

A novel PET/computed tomography method has been introduced recently for the quantification of organ-specific dietary fatty acid uptake and partitioning in most organs of the human body using oral administration of ^{18}FTHA (Fig. 2) (30). Orally administered ^{18}FTHA reaches the circulation almost exclusively in chylomicron triglycerides and is then taken up by most tissues and partly recycled in circulation in the form of NEFA by adipose tissues and VLDL triglycerides by the liver, as expected for a long-chain dietary fatty acid (30). ^{18}FTHA is taken up in tissues at a similar rate as palmitate (25, 58) and is trapped in oxidative and nonoxidative cellular pathways (9), therefore allowing the progressive accumulation of this tracer to determine organ-specific dietary fatty acid partitioning. The PET oral ^{18}FTHA method has shown peak dietary fatty acid uptake between 3 and 5 h after a meal in most organs (30), including the liver—a finding that fits well with those from the ^{13}C-MRS method described in the preceding paragraph (34). This novel technique has also demonstrated reduced dietary fatty acid partitioning per volume of central adipose tissues in prediabetes (28, 31)—a finding that is in line with those demonstrated using classical tracer methods with biopsies or arteriovenous gradient (7, 24, 39, 65). In addition, PET imaging allowed the simultaneous demonstration of normal skeletal muscle and liver but increased dietary fatty acid partitioning in the heart of prediabetic subjects (28, 31). Increased cardiac partitioning of dietary fatty acids in prediabetes is associated with reduced left ventricular function (31) and insulin resistance (42) and occurs via increased chylomicron transport in men and via increased adipose tissue spillover of NEFA in women (28). Excessive cardiac dietary fatty acid uptake and partitioning and subclinical reduction in left ventricular function are corrected by weight loss for over 1 yr following lifestyle modification (32) but not after 7 days of a hypocaloric, low-fat diet (43).

The recent application of this technique during acute cold exposure in healthy subjects, before and after prolonged cold acclimation, has demonstrated, for the first time, brown adipose tissue dietary fatty acid use in humans (5). In the later study, it was shown that brown adipose tissue can use only ~1% of dietary fatty acids even after prolonged cold acclimation that enhances the brown adipose tissue oxidative metabolism, demonstrating the limited role of this tissue for dietary fatty acid clearance in humans.

MOLECULAR IMAGING OF POSTPRANDIAL TISSUE OXIDATIVE METABOLISM

As mentioned above, next to ^{1}H- and ^{13}C-MRS, ^{31}P-MRS is also possible (Fig. 3), enabling the quantification of high-energy metabolites, such as nucleoside triphosphate (ATP and GTP). With the use of this method, it was shown that a high-fat, high-energetic meal tends to increase mean nucleoside triphosphate concentrations in healthy subjects by 6%, suggesting an increase of hepatic ATP energy reserves upon meal consumption. The physiological implications of these findings are not completely clear yet, although evidently, sufficient ATP availability is a prerequisite for many postprandial processes, including glycogen synthesis. Interestingly, ATP concentrations decreased in response to fructose ingestion in the liver during the first 50 min after ingestion (3), and the time until ATP reserves were depleted was related to body mass index, with the leaner subjects showing a slower decrease in ATP (4). The underlying mechanism of this fructose-induced ATP decrease in the liver remains to be elucidated, although the phenomenon may be indicative of the ATP use by fructose-induced stimulation of neoglucogenesis and de novo lipogenesis (59). ^{11}C-Acetate PET has also been used in the postprandial state, demonstrating increased cardiac but normal liver oxidative metabolism in subjects with prediabetes (31). The postprandial skeletal muscle oxidative metabolism was demonstrated similar to healthy subjects in patients with type 2 diabetes by ^{11}C-acetate PET (29). The later study also showed that reduction of muscle blood flow in type 2 diabetes is associated with reduced muscle fractional extraction of plasma NEFA determined by intravenous injection of ^{18}FTHA with PET. Interestingly, net postprandial muscle NEFA uptake was nevertheless normal in these patients, because higher circulating NEFA compensates for the reduction in muscle NEFA fractional extraction (29).

FUTURE PERSPECTIVES

PET and MRI/MRS now offer extended capacities to investigate the postprandial metabolism in physiological and pathological conditions. These two modalities have obvious complementary strengths. PET has unsurpassed versatility and sensitivity for the quantification of tissue in- and outflow of

energy substrates, whereas MRI/MRS has the outstanding capacity for noninvasive quantification of tissue metabolic pools and composition. The recent advances in hybrid PET/MRI, which offer the capacity for simultaneous PET and MRS measures, will open novel windows on the intricate, multiorgan metabolic abnormalities at play in the development of chronic diseases, such as diabetes and cardiovascular disorders.

GRANTS

A. C. Carpentier is the recipient of the GlaxoSmithKline Chair in Diabetes of the Université de Sherbrooke. The Centre de Recherche du Centre Hospitalier Universitaire de Sherbrooke is funded by the Fonds de Recherche du Québec–Santé.

DISCLOSURES

No conflicts of interest, financial or otherwise, are declared by the authors.

AUTHOR CONTRIBUTIONS

V.B.S-H. and A.C.C. prepared figures; V.B.S-H. and A.C.C. drafted manuscript; V.B.S-H. and A.C.C. edited and revised manuscript; V.B.S-H. and A.C.C. approved final version of manuscript.

REFERENCES

1. **American Diabetes Association.** 2. Classification and diagnosis of diabetes. *Diabetes Care* 39, *Suppl* 1: S13–S22, 2016. doi:10.2337/dc16-S005.
2. **Bassil M, Marliss EB, Morais JA, Pereira S, Chevalier S, Gougeon R.** Postprandial hyperaminoacidaemia overcomes insulin resistance of protein anabolism in men with type 2 diabetes. *Diabetologia* 54: 648–656, 2011. doi:10.1007/s00125-010-1980-9.
3. **Bawden S, Stephenson M, Falcone Y, Lingaya M, Ciampi E, Hunter K, Bligh F, Schirra J, Taylor M, Morris P, Macdonald I, Gowland P, Marciani L, Aithal GP.** Increased liver fat and glycogen stores after consumption of high versus low glycaemic index food: a randomized crossover study. *Diabetes Obes Metab* 19: 70–77, 2017. doi:10.1111/dom.12784.
4. **Bawden SJ, Stephenson MC, Ciampi E, Hunter K, Marciani L, Macdonald IA, Aithal GP, Morris PG, Gowland PA.** Investigating the effects of an oral fructose challenge on hepatic ATP reserves in healthy volunteers: A (31)P MRS study. *Clin Nutr* 35: 645–649, 2016. doi:10.1016/j.clnu.2015.04.001.
5. **Blondin DP, Tingelstad HC, Noll C, Frisch F, Phoenix S, Guérin B, Turcotte EE, Richard D, Haman F, Carpentier AC.** Dietary fatty acid metabolism of brown adipose tissue in cold-acclimated men. *Nat Commun* 8: 14146, 2017. doi:10.1038/ncomms14146.
6. **Bugger H, Abel ED.** Molecular mechanisms of diabetic cardiomyopathy. *Diabetologia* 57: 660–671, 2014. doi:10.1007/s00125-014-3171-6.
7. **Carpentier AC, Labbe SM, Grenier-Larouche T, Noll C.** Abnormal dietary fatty acid metabolic partitioning in insulin resistance and type 2 diabetes. *Clin Lipidol* 6: 703–716, 2011. doi:10.2217/clp.11.60.
8. **Chen KY, Cypess AM, Laughlin MR, Haft CR, Hu HH, Bredella MA, Enerbäck S, Kinahan PE, Lichtenbelt W, Lin FI, Sunderland JJ, Virtanen KA, Wahl RL.** Brown adipose reporting criteria in imaging studies (BARCIST 1.0): recommendations for standardized FDG-PET/CT experiments in humans. *Cell Metab* 24: 210–222, 2016. doi:10.1016/j.cmet.2016.07.014.
9. **Ci X, Frisch F, Lavoie F, Germain P, Lecomte R, van Lier JE, Bénard F, Carpentier AC.** The effect of insulin on the intracellular distribution of 14(R,S)-[18F]fluoro-6-thia-heptadecanoic acid in rats. *Mol Imaging Biol* 8: 237–244, 2006. doi:10.1007/s11307-006-0042-7.
10. **Cobelli C, Dalla Man C, Toffolo G, Basu R, Vella A, Rizza R.** The oral minimal model method. *Diabetes* 63: 1203–1213, 2014. doi:10.2337/db13-1198.
11. **Croteau E, Lavallée E, Labbe SM, Hubert L, Pifferi F, Rousseau JA, Cunnane SC, Carpentier AC, Lecomte R, Bénard F.** Image-derived input function in dynamic human PET/CT: methodology and validation with 11C-acetate and 18F-fluorothioheptadecanoic acid in muscle and 18F-fluorodeoxyglucose in brain. *Eur J Nucl Med Mol Imaging* 37: 1539–1550, 2010. doi:10.1007/s00259-010-1443-z.
12. **Cypess AM, Lehman S, Williams G, Tal I, Rodman D, Goldfine AB, Kuo FC, Palmer EL, Tseng YH, Doria A, Kolodny GM, Kahn CR.** Identification and importance of brown adipose tissue in adult humans. *N Engl J Med* 360: 1509–1517, 2009. doi:10.1056/NEJMoa0810780.
13. **de Jong HW, Rijzewijk LJ, Lubberink M, van der Meer RW, Lamb HJ, Smit JW, Diamant M, Lammertsma AA.** Kinetic models for analysing myocardial [(11)C]palmitate data. *Eur J Nucl Med Mol Imaging* 36: 966–978, 2009. doi:10.1007/s00259-008-1035-3.
14. **Demeure F, Hanin FX, Bol A, Vincent MF, Pouleur AC, Gerber B, Pasquet A, Jamar F, Vanoverschelde JL, Vancraeynest D.** A randomized trial on the optimization of 18F-FDG myocardial uptake suppression: implications for vulnerable coronary plaque imaging. *J Nucl Med* 55: 1629–1635, 2014. doi:10.2967/jnumed.114.138594.
15. **Ferrannini E, Baldi S, Frascerra S, Astiarraga B, Heise T, Bizzotto R, Mari A, Pieber TR, Muscelli E.** Shift to fatty substrate utilization in response to sodium-glucose cotransporter 2 inhibition in subjects without diabetes and patients with type 2 diabetes. *Diabetes* 65: 1190–1195, 2016. doi:10.2337/db15-1356.
16. **Hakkarainen A, Lundbom J, Tuominen EK, Taskinen MR, Pietiläinen KH, Lundbom N.** Measuring short-term liver metabolism noninvasively: postprandial and post-exercise ^{1}H and ^{31}P MR spectroscopy. *MAGMA* 28: 57–66, 2015. doi:10.1007/s10334-014-0450-7.
17. **Hällsten K, Virtanen KA, Lönnqvist F, Janatuinen T, Turiceanu M, Rönnemaa T, Viikari J, Lehtimäki T, Knuuti J, Nuutila P.** Enhancement of insulin-stimulated myocardial glucose uptake in patients with type 2 diabetes treated with rosiglitazone. *Diabet Med* 21: 1280–1287, 2004. doi:10.1111/j.1464-5491.2004.01332.x.
18. **Herman-Edelstein M, Scherzer P, Tobar A, Levi M, Gafter U.** Altered renal lipid metabolism and renal lipid accumulation in human diabetic nephropathy. *J Lipid Res* 55: 561–572, 2014. doi:10.1194/jlr.P040501.
19. **Hirvonen J, Virtanen KA, Nummenmaa L, Hannukainen JC, Honka MJ, Bucci M, Nesterov SV, Parkkola R, Rinne J, Iozzo P, Nuutila P.** Effects of insulin on brain glucose metabolism in impaired glucose tolerance. *Diabetes* 60: 443–447, 2011. doi:10.2337/db10-0940.
20. **Iozzo P, Bucci M, Roivainen A, Någren K, Järvisalo MJ, Kiss J, Guiducci L, Fielding B, Naum AG, Borra R, Virtanen K, Savunen T, Salvadori PA, Ferrannini E, Knuuti J, Nuutila P.** Fatty acid metabolism in the liver, measured by positron emission tomography, is increased in obese individuals. *Gastroenterology* 139: 846–856, 2010. doi:10.1053/j.gastro.2010.05.039.
21. **Iozzo P, Geisler F, Oikonen V, Mäki M, Takala T, Solin O, Ferrannini E, Knuuti J, Nuutila P; 18F-FDG PET Study.** Insulin stimulates liver glucose uptake in humans: an 18F-FDG PET Study. *J Nucl Med* 44: 682–689, 2003.
22. **Iozzo P, Hallsten K, Oikonen V, Virtanen KA, Kemppainen J, Solin O, Ferrannini E, Knuuti J, Nuutila P.** Insulin-mediated hepatic glucose uptake is impaired in type 2 diabetes: evidence for a relationship with glycemic control. *J Clin Endocrinol Metab* 88: 2055–2060, 2003. doi:10.1210/jc.2002-021446.
23. **Iozzo P, Viljanen A, Guzzardi MA, Laine H, Honka MJ, Ferrannini E, Nuutila P.** The interaction of blood flow, insulin, and bradykinin in regulating glucose uptake in lower-body adipose tissue in lean and obese subjects. *J Clin Endocrinol Metab* 97: E1192–E1196, 2012. doi:10.1210/jc.2011-3245.
24. **Jensen MD, Sarr MG, Dumesic DA, Southorn PA, Levine JA.** Regional uptake of meal fatty acids in humans. *Am J Physiol Endocrinol Metab* 285: E1282–E1288, 2003. doi:10.1152/ajpendo.00220.2003.
25. **Knuuti J, Takala TO, Någren K, Sipilä H, Turpeinen AK, Uusitupa MI, Nuutila P.** Myocardial fatty acid oxidation in patients with impaired glucose tolerance. *Diabetologia* 44: 184–187, 2001. doi:10.1007/s001250051597.
26. **Knuuti MJ, Mäki M, Yki-Järvinen H, Voipio-Pulkki LM, Härkönen R, Haaparanta M, Nuutila P.** The effect of insulin and FFA on myocardial glucose uptake. *J Mol Cell Cardiol* 27: 1359–1367, 1995. doi:10.1006/jmcc.1995.0129.
27. **Knuuti MJ, Nuutila P, Ruotsalainen U, Saraste M, Härkönen R, Ahonen A, Teräs M, Haaparanta M, Wegelius U, Haapanen A, et al.** Euglycemic hyperinsulinemic clamp and oral glucose load in stimulating myocardial glucose utilization during positron emission tomography. *J Nucl Med* 33: 1255–1262, 1992.
28. **Kunach M, Noll C, Phoenix S, Guérin B, Baillargeon JP, Turcotte EE, Carpentier AC.** Effect of sex and impaired glucose tolerance on organ-specific dietary fatty acid Metabolism in humans. *Diabetes* 64: 2432–2441, 2015. doi:10.2337/db14-1166.
29. **Labbé SM, Croteau E, Grenier-Larouche T, Frisch F, Ouellet R, Langlois R, Guérin B, Turcotte EE, Carpentier AC.** Normal postpran-

dial nonesterified fatty acid uptake in muscles despite increased circulating fatty acids in type 2 diabetes. *Diabetes* 60: 408–415, 2011. doi:10.2337/db10-0997.

30. **Labbé SM, Grenier-Larouche T, Croteau E, Normand-Lauzière F, Frisch F, Ouellet R, Guérin B, Turcotte EE, Carpentier AC.** Organ-specific dietary fatty acid uptake in humans using positron emission tomography coupled to computed tomography. *Am J Physiol Endocrinol Metab* 300: E445–E453, 2011. doi:10.1152/ajpendo.00579.2010.
31. **Labbé SM, Grenier-Larouche T, Noll C, Phoenix S, Guérin B, Turcotte EE, Carpentier AC.** Increased myocardial uptake of dietary fatty acids linked to cardiac dysfunction in glucose-intolerant humans. *Diabetes* 61: 2701–2710, 2012. doi:10.2337/db11-1805.
32. **Labbé SM, Noll C, Grenier-Larouche T, Kunach M, Bouffard L, Phoenix S, Guérin B, Baillargeon JP, Langlois MF, Turcotte EE, Carpentier AC.** Improved cardiac function and dietary fatty acid metabolism after modest weight loss in subjects with impaired glucose tolerance. *Am J Physiol Endocrinol Metab* 306: E1388–E1396, 2014. doi:10.1152/ajpendo.00638.2013.
33. **Lerche S, Brock B, Rungby J, Bøtker HE, Møller N, Rodell A, Bibby BM, Holst JJ, Schmitz O, Gjedde A.** Glucagon-like peptide-1 inhibits blood-brain glucose transfer in humans. *Diabetes* 57: 325–331, 2008. doi:10.2337/db07-1162.
34. **Lindeboom L, de Graaf RA, Nabuurs CI, van Ewijk PA, Hesselink MK, Wildberger JE, Schrauwen P, Schrauwen-Hinderling VB.** Quantum coherence spectroscopy to measure dietary fat retention in the liver. *JCI Insight* 1: e84671, 2016. doi:10.1172/jci.insight.84671.
35. **Lindeboom L, Nabuurs CI, Hesselink MK, Wildberger JE, Schrauwen P, Schrauwen-Hinderling VB.** Proton magnetic resonance spectroscopy reveals increased hepatic lipid content after a single high-fat meal with no additional modulation by added protein. *Am J Clin Nutr* 101: 65–71, 2015. doi:10.3945/ajcn.114.094730.
36. **Macauley M, Smith FE, Thelwall PE, Hollingsworth KG, Taylor R.** Diurnal variation in skeletal muscle and liver glycogen in humans with normal health and type 2 diabetes. *Clin Sci (Lond)* 128: 707–713, 2015. doi:10.1042/CS20140681.
37. **Magkos F, Bradley D, Eagon JC, Patterson BW, Klein S.** Effect of Roux-en-Y gastric bypass and laparoscopic adjustable gastric banding on gastrointestinal metabolism of ingested glucose. *Am J Clin Nutr* 103: 61–65, 2016. doi:10.3945/ajcn.115.116111.
38. **McGavock JM, Victor RG, Unger RH, Szczepaniak LS; American College of Physicians and the American Physiological Society.** Adiposity of the heart, revisited. *Ann Intern Med* 144: 517–524, 2006. doi:10.7326/0003-4819-144-7-200604040-00011.
39. **McQuaid SE, Hodson L, Neville MJ, Dennis AL, Cheeseman J, Humphreys SM, Ruge T, Gilbert M, Fielding BA, Frayn KN, Karpe F.** Downregulation of adipose tissue fatty acid trafficking in obesity: a driver for ectopic fat deposition? *Diabetes* 60: 47–55, 2011. doi:10.2337/db10-0867.
40. **McQuaid SE, Manolopoulos KN, Dennis AL, Cheeseman J, Karpe F, Frayn KN.** Development of an arterio-venous difference method to study the metabolic physiology of the femoral adipose tissue depot. *Obesity (Silver Spring)* 18: 1055–1058, 2010. doi:10.1038/oby.2009.486.
41. **Meikle SR, Kench P, Kassiou M, Banati RB.** Small animal SPECT and its place in the matrix of molecular imaging technologies. *Phys Med Biol* 50: R45–R61, 2005. doi:10.1088/0031-9155/50/22/R01.
42. **Noll C, Carpentier AC.** Dietary fatty acid metabolism in prediabetes. *Curr Opin Lipidol* 28: 1–10, 2017.
43. **Noll C, Kunach M, Frisch F, Bouffard L, Dubreuil S, Jean-Denis F, Phoenix S, Cunnane SC, Guérin B, Turcotte EE, Carpentier AC.** Seven-day caloric and saturated fat restriction increases myocardial dietary fatty acid partitioning in impaired glucose-tolerant subjects. *Diabetes* 64: 3690–3699, 2015. doi:10.2337/db15-0337.
44. **Normand-Lauzière F, Frisch F, Labbé SM, Bherer P, Gagnon R, Cunnane SC, Carpentier AC.** Increased postprandial nonesterified fatty acid appearance and oxidation in type 2 diabetes is not fully established in offspring of diabetic subjects. *PLoS One* 5: e10956, 2010. doi:10.1371/journal.pone.0010956.
45. **Nuutila P, Koivisto VA, Knuuti J, Ruotsalainen U, Teräs M, Haaparanta M, Bergman J, Solin O, Voipio-Pulkki LM, Wegelius U.** Glucose-free fatty acid cycle operates in human heart and skeletal muscle in vivo. *J Clin Invest* 89: 1767–1774, 1992. doi:10.1172/JCI115780.
46. **Nuutila P, Mäki M, Laine H, Knuuti MJ, Ruotsalainen U, Luotolahti M, Haaparanta M, Solin O, Jula A, Koivisto VA.** Insulin action on heart and skeletal muscle glucose uptake in essential hypertension. *J Clin Invest* 96: 1003–1009, 1995. doi:10.1172/JCI118085.
47. **Orava J, Nuutila P, Lidell ME, Oikonen V, Noponen T, Viljanen T, Scheinin M, Taittonen M, Niemi T, Enerbäck S, Virtanen KA.** Different metabolic responses of human brown adipose tissue to activation by cold and insulin. *Cell Metab* 14: 272–279, 2011. doi:10.1016/j.cmet.2011.06.012.
48. **Osborne MT, Hulten EA, Murthy VL, Skali H, Taqueti VR, Dorbala S, DiCarli MF, Blankstein R.** Patient preparation for cardiac fluorine-18 fluorodeoxyglucose positron emission tomography imaging of inflammation. *J Nucl Cardiol* 24: 86–99, 2017.
49. **Ouellet V, Labbé SM, Blondin DP, Phoenix S, Guérin B, Haman F, Turcotte EE, Richard D, Carpentier AC.** Brown adipose tissue oxidative metabolism contributes to energy expenditure during acute cold exposure in humans. *J Clin Invest* 122: 545–552, 2012. doi:10.1172/JCI60433.
50. **Ouellet V, Routhier-Labadie A, Bellemare W, Lakhal-Chaieb L, Turcotte E, Carpentier AC, Richard D.** Outdoor temperature, age, sex, body mass index, and diabetic status determine the prevalence, mass, and glucose-uptake activity of 18F-FDG-detected BAT in humans. *J Clin Endocrinol Metab* 96: 192–199, 2011. doi:10.1210/jc.2010-0989.
51. **Patlak CS, Blasberg RG.** Graphical evaluation of blood-to-brain transfer constants from multiple-time uptake data. Generalizations. *J Cereb Blood Flow Metab* 5: 584–590, 1985. doi:10.1038/jcbfm.1985.87.
52. **Peltoniemi P, Lönnroth P, Laine H, Oikonen V, Tolvanen T, Grönroos T, Strindberg L, Knuuti J, Nuutila P.** Lumped constant for [(18)F]fluorodeoxyglucose in skeletal muscles of obese and nonobese humans. *Am J Physiol Endocrinol Metab* 279: E1122–E1130, 2000.
53. **Saito M, Okamatsu-Ogura Y, Matsushita M, Watanabe K, Yoneshiro T, Nio-Kobayashi J, Iwanaga T, Miyagawa M, Kameya T, Nakada K, Kawai Y, Tsujisaki M.** High incidence of metabolically active brown adipose tissue in healthy adult humans: effects of cold exposure and adiposity. *Diabetes* 58: 1526–1531, 2009. doi:10.2337/db09-0530.
54. **Santosa S, Jensen MD.** Adipocyte fatty acid storage factors enhance subcutaneous fat storage in postmenopausal women. *Diabetes* 62: 775–782, 2013. doi:10.2337/db12-0912.
55. **Sieber J, Jehle AW.** Free fatty acids and their metabolism affect function and survival of podocytes. *Front Endocrinol (Lausanne)* 5: 186, 2014.
56. **Sokoloff L, Reivich M, Kennedy C, Des Rosiers MH, Patlak CS, Pettigrew KD, Sakurada O, Shinohara M.** The [14C]deoxyglucose method for the measurement of local cerebral glucose utilization: theory, procedure, and normal values in the conscious and anesthetized albino rat. *J Neurochem* 28: 897–916, 1977. doi:10.1111/j.1471-4159.1977.tb10649.x.
57. **Szczepaniak LS, Victor RG, Orci L, Unger RH.** Forgotten but not gone: the rediscovery of fatty heart, the most common unrecognized disease in America. *Circ Res* 101: 759–767, 2007. doi:10.1161/CIRCRESAHA.107.160457.
58. **Takala TO, Nuutila P, Katoh C, Luotolahti M, Bergman J, Mäki M, Oikonen V, Ruotsalainen U, Grönroos T, Haaparanta M, Kapanen J, Knuuti J.** Myocardial blood flow, oxygen consumption, and fatty acid uptake in endurance athletes during insulin stimulation. *Am J Physiol Endocrinol Metab Physiol* 277: E585–E590, 1999.
59. **Tappy L, Lê KA.** Metabolic effects of fructose and the worldwide increase in obesity. *Physiol Rev* 90: 23–46, 2010. doi:10.1152/physrev.00019.2009.
60. **Tonietto M, Rizzo G, Veronese M, Fujita M, Zoghbi SS, Zanotti-Fregonara P, Bertoldo A.** Plasma radiometabolite correction in dynamic PET studies: insights on the available modeling approaches. *J Cereb Blood Flow Metab* 36: 326–339, 2016. doi:10.1177/0271678X15610585.
61. **Veronese M, Rizzo G, Bertoldo A, Turkheimer FE.** Spectral analysis of dynamic PET studies: a review of 20 years of method developments and applications. *Comput Math Methods Med* 2016: 7187541, 2016. doi:10.1155/2016/7187541.
62. **Virtanen KA, Lidell ME, Orava J, Heglind M, Westergren R, Niemi T, Taittonen M, Laine J, Savisto NJ, Enerbäck S, Nuutila P.** Functional brown adipose tissue in healthy adults. *N Engl J Med* 360: 1518–1525, 2009. doi:10.1056/NEJMoa0808949.
63. **Virtanen KA, Lönnroth P, Parkkola R, Peltoniemi P, Asola M, Viljanen T, Tolvanen T, Knuuti J, Rönnemaa T, Huupponen R, Nuutila P.** Glucose uptake and perfusion in subcutaneous and visceral adipose tissue during insulin stimulation in nonobese and obese humans. *J Clin Endocrinol Metab* 87: 3902–3910, 2002. doi:10.1210/jcem.87.8.8761.
64. **Vosselman MJ, Brans B, van der Lans AA, Wierts R, van Baak MA, Mottaghy FM, Schrauwen P, van Marken Lichtenbelt WD.** Brown

adipose tissue activity after a high-calorie meal in humans. *Am J Clin Nutr* 98: 57–64, 2013. doi:10.3945/ajcn.113.059022.

65. **Votruba SB, Mattison RS, Dumesic DA, Koutsari C, Jensen MD.** Meal fatty acid uptake in visceral fat in women. *Diabetes* 56: 2589–2597, 2007. doi:10.2337/db07-0439.
66. **Vrieze A, Schopman JE, Admiraal WM, Soeters MR, Nieuwdorp M, Verberne HJ, Holleman F.** Fasting and postprandial activity of brown adipose tissue in healthy men. *J Nucl Med* 53: 1407–1410, 2012. doi:10.2967/jnumed.111.100701.
67. **Zingaretti MC, Crosta F, Vitali A, Guerrieri M, Frontini A, Cannon B, Nedergaard J, Cinti S.** The presence of UCP1 demonstrates that metabolically active adipose tissue in the neck of adult humans truly represents brown adipose tissue. *FASEB J* 23: 3113–3120, 2009. doi:10.1096/fj.09-133546.